Report

Cell Reports

A Cell Engineering Strategy to Enhance the Safety of Stem Cell Therapies

Graphical Abstract

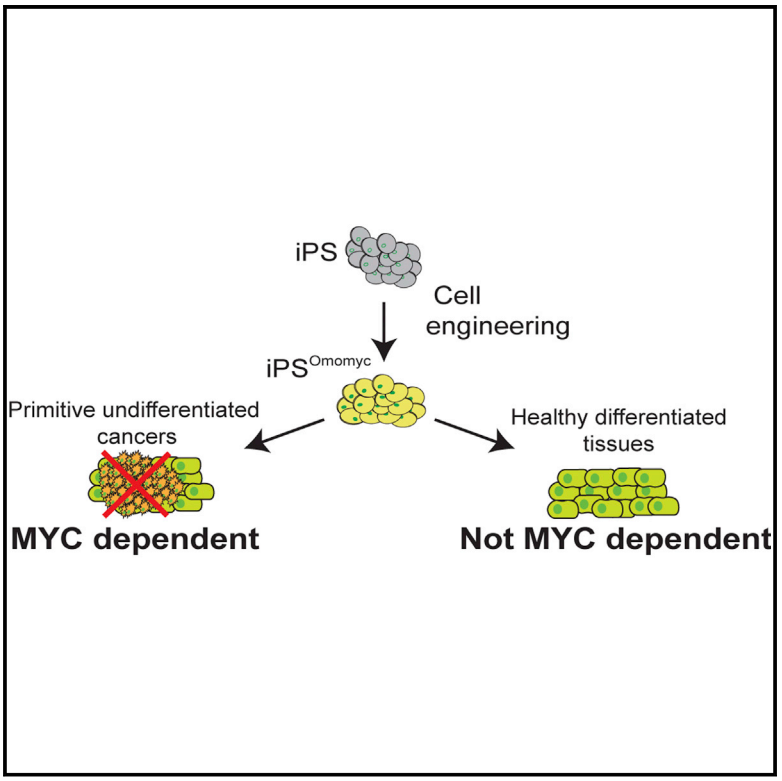

Authors

Elisa Oricchio, Eirini P. Papapetrou, ..., Lorenz Studer, Hans-Guido Wendel

Correspondence

wendelh@mskcc.org

In Brief

The risk of malignancies arising from iPSC-derived tissues is a critical concern in stem cell therapies. Oricchio et al. report an iPSC engineering strategy that exploits cancer dependence on MYC and can be activated should a malignancy arise. They further report that MYC blockade disrupts a cancer-specific feed-forward program centered on the role of PKM2 in cancer metabolism and its ability to modulate gene expression via histone H3 phosphorylation.

Highlights

Cancer and normal tissues derived from iPSCs differentially depend on MYC

MYC sustains tumor-specific metabolic and chromatin changes in iPSC-derived tumors

Engineering iPSCs with dominant-negative MYC is a therapeutic fail-safe strategy

Oricchio et al., 2014, Cell Reports 8, 1677–1685
September 25, 2014 ©2014 The Authors
http://dx.doi.org/10.1016/j.celrep.2014.08.039

Cell Reports
Report

A Cell Engineering Strategy to Enhance the Safety of Stem Cell Therapies

Elisa Oricchio,[1] Eirini P. Papapetrou,[2,7] Fabien Lafaille,[3] Yosif M. Ganat,[3] Sonja Kriks,[3] Ana Ortega-Molina,[1] Willie H. Mark,[4] Julie Teruya-Feldstein,[5] Jason T. Huse,[5] Victor Reuter,[5] Michel Sadelain,[2,6] Lorenz Studer,[2,3] and Hans-Guido Wendel[1,*]

[1]Cancer Biology & Genetics Program, Memorial Sloan-Kettering Cancer Center, New York, NY 10065, USA
[2]Center for Cell Engineering, Memorial Sloan-Kettering Cancer Center, New York, NY 10065, USA
[3]Developmental Biology Program, Memorial Sloan-Kettering Cancer Center, New York, NY 10065, USA
[4]Mouse Genetics Core, Memorial Sloan-Kettering Cancer Center, New York, NY 10065, USA
[5]Department of Pathology, Memorial Sloan-Kettering Cancer Center, New York, NY 10065, USA
[6]Molecular Pharmacology and Chemistry Program, Memorial Sloan-Kettering Cancer Center, New York, NY 10065, USA
[7]Present address: Oncological Sciences, Mount Sinai Hospital, New York, NY 10029, USA
*Correspondence: wendelh@mskcc.org
http://dx.doi.org/10.1016/j.celrep.2014.08.039

SUMMARY

The long-term risk of malignancy associated with stem cell therapies is a significant concern in the clinical application of this exciting technology. We report a cancer-selective strategy to enhance the safety of stem cell therapies. Briefly, using a cell engineering approach, we show that aggressive cancers derived from human or murine induced pluripotent stem cells (iPSCs) and embryonic stem cells (ESCs) are strikingly sensitive to temporary *MYC* blockade. On the other hand, differentiated tissues derived from human or mouse iPSCs can readily tolerate temporary *MYC* inactivation. In cancer cells, endogenous MYC is required to maintain the metabolic and epigenetic functions of the embryonic and cancer-specific pyruvate kinase M2 isoform (PKM2). In summary, our results implicate PKM2 in cancer's increased MYC dependence and indicate dominant MYC inhibition as a cancer-selective fail-safe for stem cell therapies.

INTRODUCTION

Tissues derived from pluripotent stem cells (PSCs) cells have great potential in regenerative medicine and can, in principle, replace any differentiated tissue (Hanna et al., 2007; Takahashi and Yamanaka, 2006). Recent successes include the generation of retinal cells (Osakada et al., 2009), functional liver tissue (Takebe et al., 2013), and dopaminergic neurons (Kriks et al., 2011). These strategies are approaching clinical testing, but the risk of iatrogenic malignancy remains a significant concern (Goldring et al., 2011; Lee et al., 2013). For example, cancers develop with increased frequency in induced pluripotent stem (iPS) cell-chimeric animals (Carey et al., 2010; Okita et al., 2007; Stadtfeld et al., 2010b), and neuronal tumors occur in primates injected with PSC-derived neurogenic cells (Doi et al., 2012). Most dramatically, an ataxia telangiectasia patient developed multifocal aggressive brain cancer following administration of neurogenic stem cells (Amariglio et al., 2009). These citations illustrate a need for effective and cancer-selective fail-safe mechanisms.

The causes of malignancy are not entirely clear. Reactivation of reprogramming factors, especially the *MYC* oncogene, has been implicated (Okita et al., 2007). However, cancers also occurred, albeit with lower frequency, when *MYC* was omitted form reprogramming protocols (Miura et al., 2009; Nakagawa et al., 2008; Werbowetski-Ogilvie et al., 2009). Notably, malignant and pluripotent cells show increased genomic instability, frequent and nonrandom chromosomal aberrations, and recurrent inactivation of canonical tumor-suppressor genes (Hussein et al., 2011; Marión et al., 2009; Mayshar et al., 2010). These findings suggest that initial barriers to transformation may be fortuitously inactivated in PSC and derived tissues.

Improved reprogramming procedures have greatly reduced, but not eliminated, the risk of cancer (Lee et al., 2013). These include nonintegrating and excisable vectors, the exclusion of *MYC*, and reprogramming by RNA, protein, or small molecules (Carey et al., 2010; Kaji et al., 2009; Stadtfeld et al., 2010a; Wernig et al., 2008). Additional strategies seek to purge residual PSCs, genomic surveys for somatic mutations, and conventional suicide genes (Choo et al., 2008; Tan et al., 2009). In this study, we explore a strategy based on recent insight into cancer's "oncogene dependence" (Jain et al., 2002; Soucek et al., 2008; Weinstein, 2002). We show that introduction of a dominant-negative *MYC* construct and temporary MYC inactivation can destroy aggressive iPS and embryonic stem (ES) cell-derived cancers while sparing healthy PSC-derived tissues.

RESULTS

To explore the MYC dependence of PSC-derived tissues, we introduced a dominant-negative MYC allele into karyotypically

normal human and murine PSCs (Figure 1A). Briefly, Omomyc^{ER} is an inducible dominant-negative *MYC* allele that is uniquely able to form inactive dimers with all three endogenous MYC proteins and does not bind other helix-loop-helix factors (Savino et al., 2011; Soucek et al., 1998). We reprogrammed human and murine fibroblasts using a single excisable polycistronic construct or four separate vectors, respectively (Papapetrou et al., 2011). We confirmed reprogramming by immunofluorescence for NANOG and showed loss of the exogenous construct by fluorescence-activated cell sorting and PCR (Figures S1A–S1C). We isolated karyotypically normal clones and introduced Omomyc along with a citrine reporter into both human iPS and murine iPS and ESCs (Figures S1D–S1E).

Murine iPSCs deficient for the p53 tumor suppressor give rise to aggressive embryonal carcinomas. Briefly, the *p53* tumor suppressor restricts reprogramming and *p53*-deficient murine fibroblast formed iPSC colonies faster than wild-type cells (Figure S1F) (Hong et al., 2009; Marión et al., 2009). Upon transplantation, the $p53^{-/-}$ iPSCs rapidly formed aggressive cancers ($p53^{+/+}$: n = 5; $p53^{-/-}$: n = 5; latency to 1 cm^3 tumor $p < 0.001$) (Figure S1G). Pathologically, these cancers resembled primitive embryonal carcinomas (EC), composed of immature OCT4- and CD30-negative tissues with some SALL4 expression (28% ± 11% [mean ± SD]), a high proliferation index by Ki67 (34.6% ± 6%), and little apoptosis by TUNEL (14.2% ± 10%) (Figure S1H). Notably, the human *MYC* transgene was not reactivated in these cancers, and instead we observed elevated expression of the endogenous *Myc* mRNA (Figure S1I).

Temporary MYC blockade produced dramatic regression in aggressive iPSC-derived embryonal carcinomas. We initiated tamoxifen (TAM) treatment when tumors reached 1 cm^3 (TAM: 10 mg/ml, alternate days for 2 weeks). This treatment caused the Omomyc^{ER}-expressing cancers (left flank) to collapse whereas control tumors (right flank) continued to grow (n_{Omo} = 5, $n_{Control}$ = 5, $p < 0.005$) (Figures 1B–1D). After TAM treatment, we retrieved a residual cystic mass containing cartilaginous material, large areas of TUNEL-positive apoptosis, and some SALL4-positive and Ki67-negative cells indicating yolk sac differentiation and absence of proliferation (Omomyc^{ER} versus control: SALL4: 92.3% ± 19% versus 28.7% ± 14%, $p < 0.05$; TUNEL: 41.2% ± 13% versus 14.2% ± 10%; $p < 0.05$; Ki67: 34.6% ± 6% versus 24.2% ± 10%) (Figure 1E; Figure S1J).

We confirmed these observations using murine ESCs expressing a p53 short-hairpin RNA to ensure these results did not reflect specific properties of the iPSCs. Briefly, cancers derived from ES cells were pathologically indistinguishable from cancers derived from iPSCs (Figures S1K–S1M). They responded in exactly the same manner to Omomyc^{ER} activation (Figures S1N–S1P). Hence, aggressive and p53-deficient cancers derived from PSCs strictly depend on the continuous activity of endogenous MYC.

Next, we tested the effect of MYC inactivation on well-differentiated, benign teratomas. Briefly, p53 wild-type iPS and ESCs give rise to typical teratomas composed of several different germ cell layers including cartilage and neuronal and glial tissues that lacked the pluripotency markers CD30 and OCT4 and contained a few SALL4-positive cells indicating early yolk sac differentiation (11.8% ± 7% [mean ± SD]) (Figures S1Q, S1U, and S1V). As seen with the aggressive embryonal carcinomas, the iPSC-derived teratomas showed no expression of the exogenous MYC, and instead the endogenous Myc mRNA was modestly increased (Figures S1R and S1S). Omomyc^{ER} induction using the same protocol as before produced no measurable effect on iPS or ESC-derived teratomas (n_{Omo} = 6, $n_{control}$ = 6; p = 0.7) (Figures S1T, S1U, and S1W–S1Z) and showed no difference in proliferation or apoptosis by Ki67 and TUNEL stains, respectively (control versus Omomyc: Ki67: 8.7% ± 5% versus 9.1% ± 2.5%; $p > 0.05$; TUNEL 5.6% ± 3.6% versus 3.6% ± 2%; $p > 0.05$). Hence, differentiated teratomas no longer depend on MYC and are insensitive to MYC blockade.

Potentially, MYC blockade can be used to purge in vitro cultures form residual iPSCs and to prevent tumor growth. To test these possibilities we first activated omomyc in iPSC cultures and observed rapid induction of cell death consistent with the notion that MYC is required to maintain these pluripotent cells (Figures S1A1 and S1B1) (Cartwright et al., 2005). We also tested whether Omomyc might be able to delay or prevent tumor formation in vivo. Briefly, we activated Omomyc^{ER} shortly following transplantation, and this could significantly reduce teratoma formation in vivo (iPS Omomyc^{ER} untreated n = 4, iPS Omomyc^{ER} tamoxifen [10 mg/ml] n = 4, p = 0.02) (Figures S1C1 and S1D1). Hence, Omomyc^{ER} can effectively purge residual tumorigenic iPSCs.

Next, we wanted to explore the effect of temporary MYC inactivation on healthy iPSC-derived tissues in vivo. We generated chimeric animals from iPSCs transduced with Omomyc^{ER} to test the effect of temporary MYC inactivation in a physiological context. Briefly, we injected two clones of karyotypically normal, iPSCs of C57B1/6J background into C57Bl/6J (B6(Cg)-$Tyr^{c\text{-}2J}$/J blastocysts and confirmed chimerism by the presence of black coat derived from donor cells. Tamoxifen treatment (TAM, 10 mg/ml on alternate days for 3 weeks) had no untoward effects on animal health, weight, or behavior (not shown) or skin and hair (Figure 1F). Omomyc^{ER}-expressing tissues were readily detectable by the coexpressed citrine reporter, and immunohistochemistry confirmed significant contributions of iPS cells expressing omomyc (iPS^{OMO}) before and after tamoxifen treatment to various organs. For example, hair follicles, dermal and epidermal structures, the upper and lower gastrointestinal tract, the kidney, red and white pulp of spleen, and thyroid gland showed persistent and extensive contribution of iPS^{OMO}-derived and citrine-positive cells and histologically intact organs after a 3-week course of systemic tamoxifen treatment (Figure 1G). Hence, temporary MYC blockade is tolerated and does not cause permanent disruption of iPSC-mosaic organs and tissues.

We now wanted to test this strategy in human iPSC-derived tissues to model a clinically relevant setting. Briefly, we engineered human iPSCs to express Omomyc^{ER} and differentiated these cells into neurogenic precursors (Rosette stage) and midbrain dopaminergic neurons according to published protocols (Chambers et al., 2009; Kriks et al., 2011). Intracerebral injection of 2×10^5 neurogenic precursors into the striatum of nonobese diabetic/severe combined immunodeficiency (NOD/SCID) animals resulted in the development of brain tumors within 4 weeks (tumor incidence: 9/9; vector n = 4 and Omomyc^{ER} n = 5) (Figure 2A). Histologically, these tumors resembled primitive

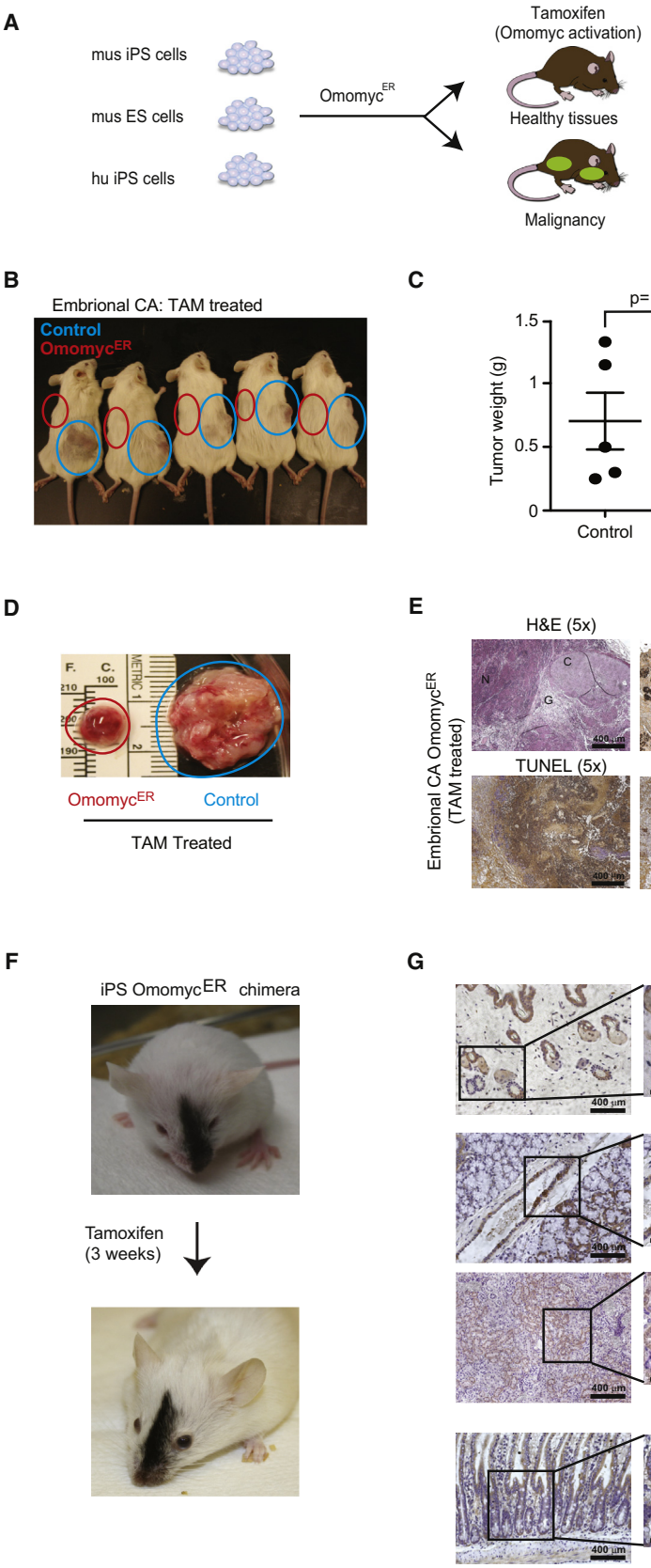

Figure 1. Aggressive Embryonal Carcinomas Are Sensitive to Omomyc^{ER} Treatment

(A) Schematic of mouse iPS (mu iPS), ES (mu ES), and human iPS (hu iPS) cells engineered with and without inducible dominant-negative *MYC* allele Omomyc^{ER}.

(B) Animals bearing embryonal carcinomas derived either from iPSCs expressing Omomyc^{ER} (red circle) or from control vector (blue circle) and treated with tamoxifen (TAM).

(C and D) Comparison of tumor weights following TAM treatment. The blue and red circles highlight the position (D) and the size (C) of the xenografted tumors. Error bars represent SDs, and the p value has been calculated by a paired t test.

(E) Histopathology of primitive embryonal carcinomas (embryonal CA) stained as indicated.

(F) Representative chimeric animal before and after a 3-week course of tamoxifen (TAM) treatment to activate the dominant-negative MYC construct in iPSC-derived tissues (the same schedule was used in tumor treatment studies).

(G) Immunohistochemical stain for citrine identifies tissues derived from Omomyc^{ER}-expressing iPSCs in different organ sites (panels from top): hair follicles, upper gastrointestinal tract and adjacent thyroid gland, kidney, lower gastrointestinal tract, and mucosal villi.

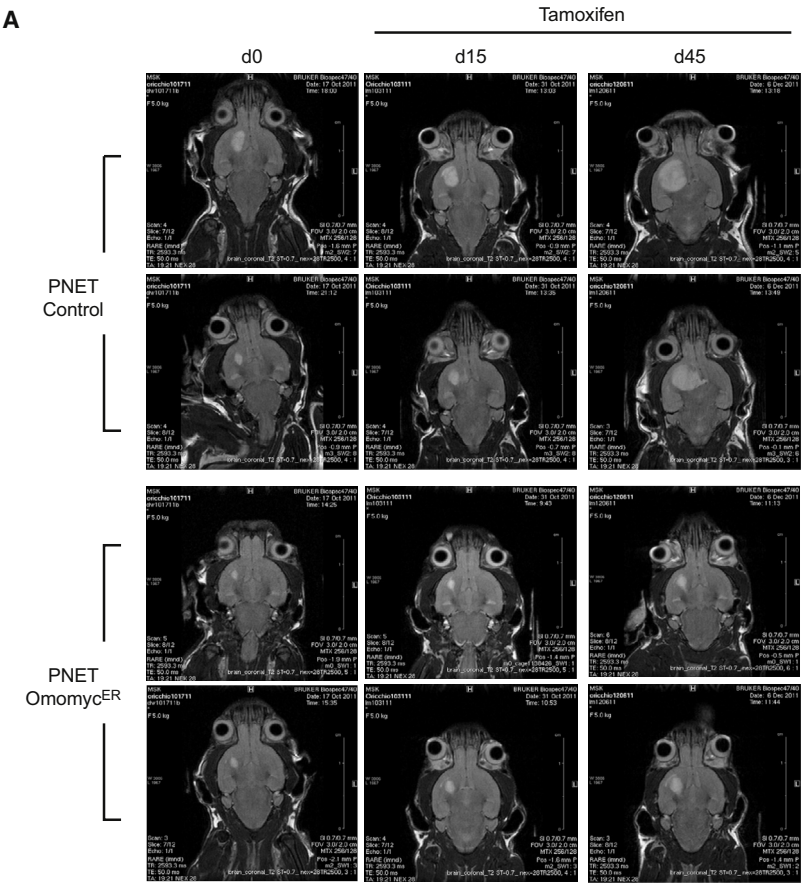

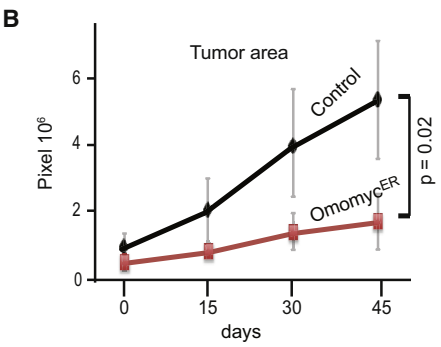

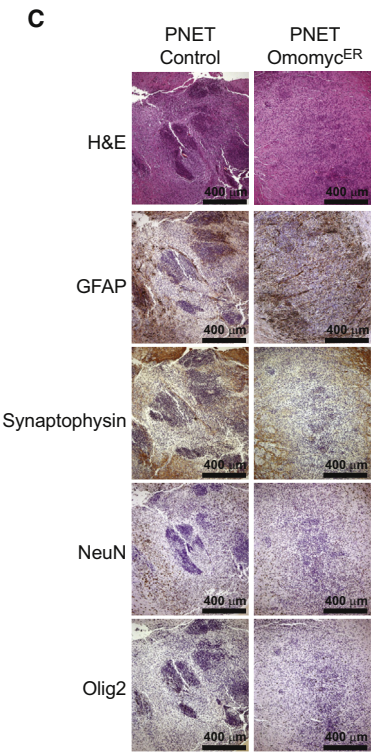

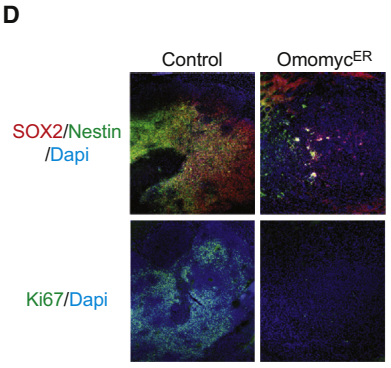

Figure 2. Primitive Neuroectodermal Tumors Derived from Human iPS Cells Respond to Omomyc^{ER} Activation In Vivo

(A) MRI of vector control (control) and Omomyc^{ER}-expressing PNETs before tamoxifen treatment and at the indicated times after treatment.

(B) Tumor size measured as pixel counts on MRI images of control and Omomyc^{ER} PNETs. Error bars represent SDs from the mean.

(C) Histology and indicated immunohistochemical stains on control and Omomyc^{ER} PNETs after tamoxifen.

(D) Immunofluorescence stains for Ki67 and SOX2/Nestin on Omomyc^{ER} and control PNETs after treatment.

neuroectodermal tumors (PNETs) with islands of highly proliferative and Ki67-positive cells, invasive spread across the brain, and expression of primitive markers (SOX2, NESTIN) in the absence of differentiation markers (OLIG2, NeuN, synaptophysin, or GFAP) (Figures S2A and S2B). Hence, we can model primitive iPSC-derived brain tumors in vivo and recapitulate the pathology previously seen in a patient treated with neurogenic precursors (Amariglio et al., 2009; Doi et al., 2012).

Omomyc^{ER} arrests the growth of brain cancers caused by human iPSC-derived neurogenic precursors. We initiated systemic tamoxifen treatment to induce the Omomyc^{ER} construct once brain tumors were diagnosed by magnetic resonance imaging (MRI) (here, "d0" represents the start of TAM treatment at 10 mg/ml, two times per week for 5 weeks). This treatment blocked the expansion of Omomyc^{ER}-expressing PNETs, while PNETs-expressing a control vector continued to grow ($n = 4$; $p = 0.02$) (Figures 2A and 2B). Histology and immunohistochemistry revealed complete disappearance of the Ki67-positive proliferative compartment of these cancers; the treatment did not alter tumor cell differentiation indicated by unchanged surface marker expression (Figures 2C and 2D). Hence, MYC blockade eliminates the growth fraction in iPSC-derived PNETs.

Next, we wondered how MYC blockade would affect differentiated midbrain dopaminergic neurons in vivo. The engraftment of 1.5×10^5 iPSC-derived neurons injected into the striatum of NOD/SCID animals was readily discernible by MRI and subsequent tamoxifen treatment (using the same schedule as above) to activate OmomycER did not affect the radiological appearance control or OmomycER-expressing neurons (Figures 3A–3D). Microscopy and immunohistochemical stains for neuronal markers (tyrosine hydroxylase, human neural cell adhesion molecule [hNCAM]) and a transcription factor characteristic of dopaminergic midbrain neurons (FoxA2) confirmed equal engraftment of morphologically intact Omomyc^{ER} and control dopaminergic neurons (Figures 3E and 3F). Together, these data reveal a differential requirement for MYC activity in iPSC-derived brain cancers (PNETs) that renders these tumors sensitive to an inhibitory MYC allele.

What may cause this differential MYC requirement between normal and malignant tissues? We examined how MYC contributes to the hallmark differences between normal neurons and malignant PNETS (Figure 4A). For example, MYC has been implicated in cancer-specific changes in glutamine metabolism and mitochondrial biology (Gao et al., 2009; Zhang et al., 2012). However, we saw only modest or no difference in expression of the glutamine transporter (*SLC1A5*) or the glutaminase enzyme (*GLS*) between differentiated neurons and PNETs (Figures 4A–4C; Figure S3A). Similarly, the ratio of mitochondrial to nuclear DNA, the expression of the mitogenesis factor *TFAM* (Li et al., 2005), or the cancer-associated uncoupling protein *UCP2* (Zhang et al., 2011) revealed no cancer-specific changes (Figures S3B–S3D).

MYC has been implicated in the Warburg effect and aerobic glucose metabolism (Dang et al., 2009). While we found no change in hexokinase expression (Figure 4D), both the pyruvate kinase isoform M2 (*PKM2*) and lactate dehydrogenase A (*LDH-A*) were strikingly increased in PNETS compared to neurons (Figures 4E and 4F). Importantly, their expression was strictly dependent on MYC, and Omomyc^{ER} activation resulted in near-complete loss of PKM2 and LDH-A mRNA and protein expression in PNETs (Figures 4G–4J; Figure S3E). In addition to its role in aerobic glycolysis, PKM2 has a surprising nuclear function and phosphorylates histone H3 to control *MYC* and *CCND1* expression (Yang et al., 2012). Indeed, we confirm this PKM2 function in Omomyc^{ER}-expressing PNETs in vivo, where TAM treatment causes rapid loss of histone H3 (T11) phosphorylation and reduction in the expression of the *c-MYC* mRNA (Figures 4K and 4L). Hence, the differential response of normal and malignant cells to MYC inactivation reflects, at least in part, the disruption of a metabolic and epigenetic feed-forward program (Figure 4M).

DISCUSSION

We report a strategy for enhancing the safe use of stem cells in regenerative medicine. The propensity of PSC-derived tissues for malignant transformation is a significant clinical concern as highlighted by recent reports of cancer development following the administration of neurogenic cells (Amariglio et al., 2009; Doi et al., 2012). Continuing improvements in reprogramming procedures, the selection of genetically suitable clones, and different purging strategies will clearly help attenuate the risk (Lee et al., 2013). We report an additional strategy that is rooted in the concept of cancer's "oncogene dependence" (Jain et al., 2002; Soucek et al., 2008; Weinstein, 2002). Specifically, the dominant-negative Omomyc^{ER} allele provides a unique tool to block transcriptional activation by all three MYC proteins (Savino et al., 2011; Soucek et al., 1998, 2002, 2008). Engineering PSCs that harbor an inducible MYC inhibitory allele provides a fail-safe mechanism that can be used to (1) purge residual iPSCs (before and after engraftment), and (2) treat aggressive cancers with a high degree of selectivity for the malignant and rapidly proliferating cells and little or no effect on differentiated tissues.

Our study also explores the causes underlying the differential MYC requirement in cancer (von Eyss and Eilers, 2011). Prior work has emphasized MYC's role maintaining angiogenesis (Sodir et al., 2011) and its ability to restrain cellular senescence or differentiation (Lin et al., 2009; Varlakhanova et al., 2011; Wu et al., 2007). Our results indicate that the differential MYC requirement reflects, at least in part, the need to maintain the expression of the cancer-specific isoforms of pyruvate kinase (PKM2) and lactate dehydrogenase (LDH-A) (Christofk et al., 2008; Clower et al., 2010; David et al., 2010; Shim et al., 1997; Vander Heiden et al., 2009). Moreover, PKM2 is required to maintain MYC expression and PKM2 loss disrupts a cancer-specific epigenetic feed-forward mechanism (Yang et al., 2012).

EXPERIMENTAL PROCEDURES

Generation and Characterization of iPS Cells

Murine iPSCs were derived from mouse embryonic fibroblasts (MEFs) infected with four lentiviral vectors (pLM-OCT4, pLM-Sox2, pLM-Myc, and pLM-Klf4) expressing OCT4, SOX2, KLF4 and MYC, plated on feeder layers of mitomycin-C-treated embryonic fibroblasts (GlobalCells) after 96 hr.

Single ESC-like colonies were picked and expanded after 10–25 days and cultivated on mitomycin-C-treated MEFs in KnockOut Dulbecco's modified

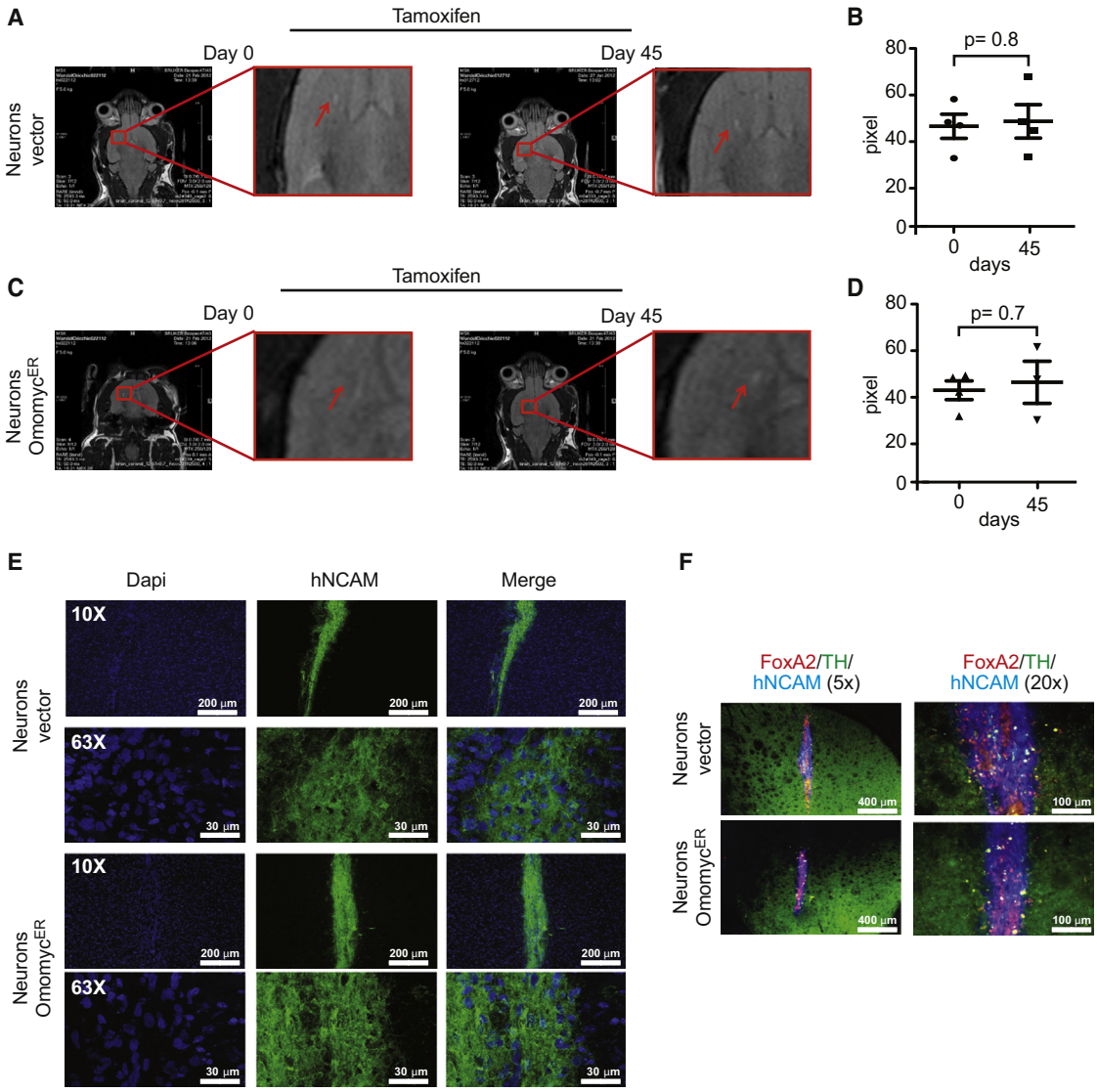

Figure 3. Human iPSC-Derived Dopaminergic Neurons Engraft In Vivo and Tolerate Omomyc^{ER} Activation

(A and C) MRI showing engraftment of control (a) and Omomyc^{ER} (c) neurons following injection into the midbrain (striatum) under tamoxifen treatment (same schedule as in tumor studies).

(B and D) Quantification of engraftment for control (B) and Omomyc^{ER}-expressing (D) neurons by MRI and pixel count to determine area of engraftment. Error bars represent SDs, and the p value has been calculated by an unpaired t test.

(E) Immunofluorescence stains of murine brain sections stained for hNCAM (green) and DAPI (blue).

(F) Immunohistochemical stains for human dopaminergic neuron markers including FOXA2, tyrosine hydroxylase, and hNCAM on control and Omomyc^{ER}-expressing neurons.

Eagle's medium with high glucose (GIBCO), supplemented with 15% fetal bovine serum (Hyclone), 0.1 mM b-mercaptoethanol, 4 mM L-glutamine, 1X Nonessential amino acids and 1000 U/ml of leukemia inhibitory factor. Media was changed every day. The human iPSC line thal5.10 was generated with a single, excisable polycistronic vector expressing OCT4, KLF4, MYC, and SOX2 (Papapetrou et al., 2011). The media were changed 24 hr later and replaced every day thereafter with human ESC media supplemented with 6 ng/ml FGF2 (R&D Systems) and 0.5 mM valproic acid (Sigma). A total of 15 to 25 days after transduction, colonies with human ESC morphology were mechanically dissociated and transferred into plates preseeded with mitomycin-C-treated MEFs (GlobalStem). Cells were thereafter passaged with dispase and expanded to establish iPSC lines.

iPSC clones were characterized by immunofluorescence using anti-Nanog Alexa 488-conjugated (eBioscience) and anti-SSEA-1 Alexa Fluor 647-conjugated (eBioscience). Gene expression of endogenous and transgenic Oct4, Myc, Sox2, and Klf4 was by TaqMan quantitative RT-PCR assay.

Tumor Analysis

A total of 1 × 10^6 iPSCs expressing omomyc^{ER} or controls were injected subcutaneously into NOD/MrkBomTac-*Prkdc*^{scid} (Taconic) mice. When the tumors were well palpable (~1 cm^3), the mice were treated with 100 µl of tamoxifen (TAM, intraperitoneal, 10 mg/ml in peanut oil). Tumors were collected 1 week after the last treatment, weighed, and fixed in 4% formaldehyde for subsequent stains including hematoxylin and eosin and

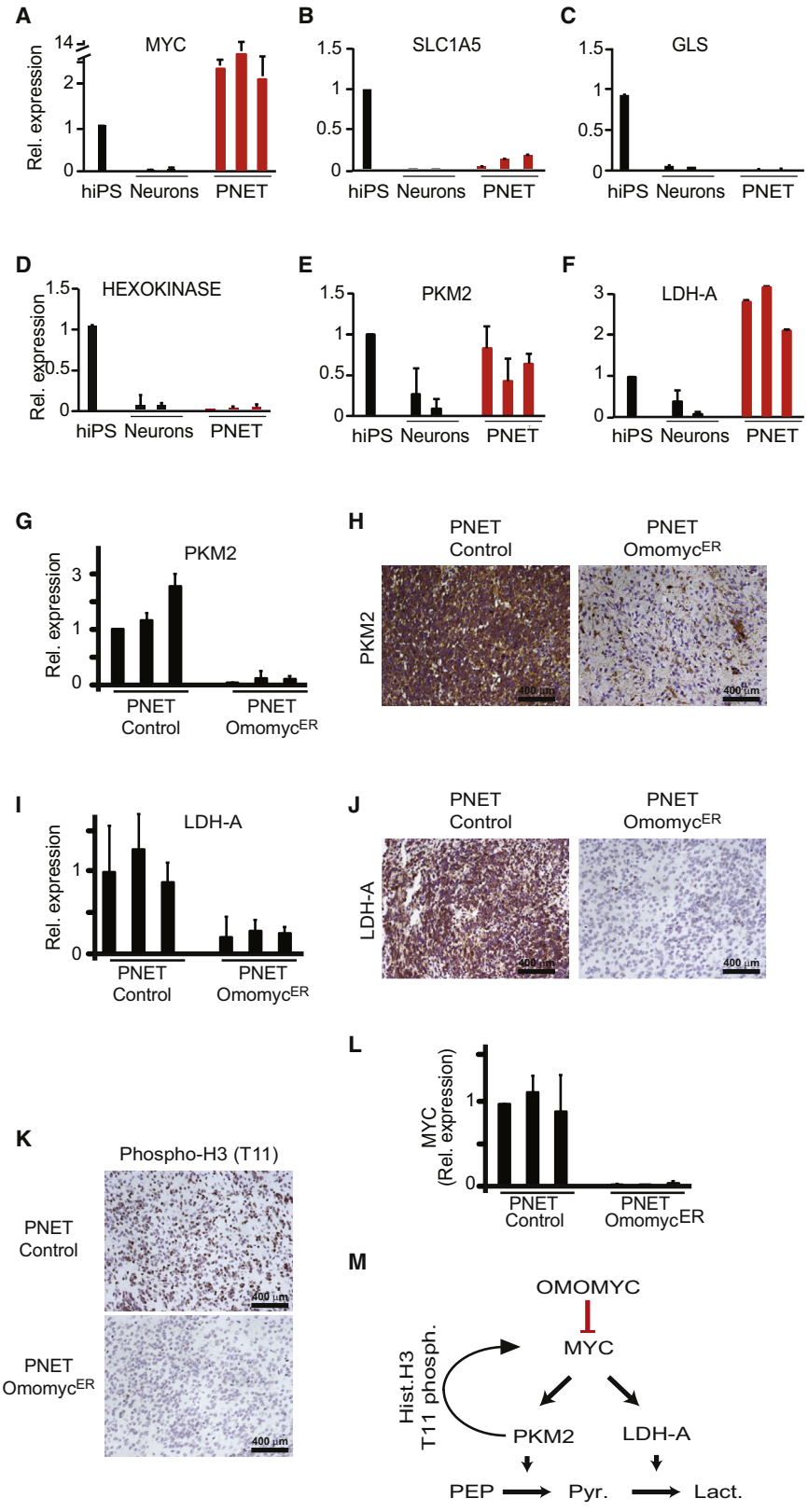

Figure 4. Omomyc^{ER}-Sensitive Changes in PKM2 and LDH-A Expression Distinguish PNETs from Differentiated Neurons

(A) Quantitative RT-PCR measuring relative expression of *MYC* in human iPSCs (hiPS), dopaminergic neurons (Neurons), and brain tumors (PNETs).

(B–F) Quantitative RT-PCR measuring relative expression of the indicated genes: glutamine transporter *SLC1A5*) (B), glutaminase (*GLS*) (C), hexokinase (D), pyruvate kinase M2 isoform (*PKM2*) (E), and lactate dehydrogenase A (*LDH-A*) (F).

(G and H) Quantitative RT-PCR (G) and immunohistochemistry (H) measuring LDH-A mRNA and protein expression in control and Omomyc^{ER} PNETs following in vivo tamoxifen treatment.

(I and J) Quantitative RT-PCR (I) and immunohistochemistry for LDH-A in control and Omomyc^{ER} PNETs following treatment.

(K) Immunohistochemical stain for histone H3 (T-11 phosphorylation) in control and Omomyc^{ER} PNETs after tamoxifen treatment in vivo.

(L) Quantitative RT-PCR measuring endogenous *MYC* expression in control and Omomyc^{ER} PNETs after tamoxifen treatment in vivo. Error bars represent SDs calculated in three independent experiments.

(M) Diagram describing that Omomyc^{ER} disrupts MYC and PKM2 dependent metabolic and transcriptional changes in cancer.

immunohistochemistry. SALL4 and OCT4 were performed on automated platforms (Ventana) per the manufacturer's instructions.

Generation of Chimeric Mice

Single-cell suspensions of exponentially growing iPSCs were used for blastocysts injection by the standard procedure. Blastocysts were obtained at day 3.5 of gestation from superovulated albino C57Bl/6J (B6(Cg)-*Tyr*$^{c-2J}$/J, Jax # 000058) female mice. For each blastocyst, an average of either 8 or 12 iPSCs was injected. After injection, blastocysts were returned to optimization medium and placed at 37°C until transferred to recipient females. A total of 10–15 injected blastocysts were transferred to each uterine horn of 2.5-day-postcoitum-pseudopregnant females. Animal studies were approved by institutional animal care and use committees.

SUPPLEMENTAL INFORMATION

Supplemental Information includes Supplemental Experimental Procedures and three figures and can be found with this article online at http://dx.doi.org/10.1016/j.celrep.2014.08.039.

AUTHOR CONTRIBUTIONS

E.O. designed and conducted the study and analyzed data; E.P., S.K., F.L., Y.G., and A.O.-M. conducted and analyzed experiments; J.T.F., V.R., and J.T.H. performed tumor pathology; W.H.M. performed blastocyst injections; L.S. and M.S. designed the study and analyzed data; and H.G.W. and E.O. designed the study and wrote the paper.

ACKNOWLEDGMENTS

We thank Gerard Evan and Laura Soucek for the Omomyc^{ER} construct; Zhimin (James) Lu, Martin Eilers, Hank Kung, and Craig Thompson for helpful discussions; D.P. Winkleman and C.C. Le for help with MRI imaging; the MSK research animal facility and the MSK Mouse Genetics Core; and the MSKCC Pathology Core Facility. This work is supported by grants from the NCI (R01-CA142798-01) and a P30 supplemental award (H.G.W.), the Leukemia Research Foundation (H.G.W.), the Louis V. Gerstner Foundation (H.G.W.), the WLBH Foundation (H.G.W.), the Society of MSKCC (H.G.W. and J.T.H.), the Starr Cancer Consortium grant I4-A410 (H.G.W.), The NYSTEM grant #C028131 (H.G.W.), NCI Carrier Developmental Award 1K99CA175179-01A1 (E.O.), a Leukemia and Lymphoma Society fellowship (A.O.-M.), the Doris Duke Charitable Foundation (J.T.H.), the Sidney Kimmel Foundation (J.T.H.), the AACR/Landon Foundation (J.T.H.), the MSKCC Brain Tumor Center (J.T.H.), MSKCC core grant NIH (P30-CA 008748) (M.H.W.), and the NINDS (R01NS066390; L.S.).

Received: March 6, 2014
Revised: July 25, 2014
Accepted: August 16, 2014
Published: September 18, 2014

REFERENCES

Amariglio, N., Hirshberg, A., Scheithauer, B.W., Cohen, Y., Loewenthal, R., Trakhtenbrot, L., Paz, N., Koren-Michowitz, M., Waldman, D., Leider-Trejo, L., et al. (2009). Donor-derived brain tumor following neural stem cell transplantation in an ataxia telangiectasia patient. PLoS Med. *6*, e1000029.

Carey, B.W., Markoulaki, S., Beard, C., Hanna, J., and Jaenisch, R. (2010). Single-gene transgenic mouse strains for reprogramming adult somatic cells. Nat. Methods *7*, 56–59.

Cartwright, P., McLean, C., Sheppard, A., Rivett, D., Jones, K., and Dalton, S. (2005). LIF/STAT3 controls ES cell self-renewal and pluripotency by a Myc-dependent mechanism. Development *132*, 885–896.

Chambers, S.M., Fasano, C.A., Papapetrou, E.P., Tomishima, M., Sadelain, M., and Studer, L. (2009). Highly efficient neural conversion of human ES and iPS cells by dual inhibition of SMAD signaling. Nat. Biotechnol. *27*, 275–280.

Choo, A.B., Tan, H.L., Ang, S.N., Fong, W.J., Chin, A., Lo, J., Zheng, L., Hentze, H., Philp, R.J., Oh, S.K., and Yap, M. (2008). Selection against undifferentiated human embryonic stem cells by a cytotoxic antibody recognizing podocalyxin-like protein-1. Stem Cells *26*, 1454–1463.

Christofk, H.R., Vander Heiden, M.G., Harris, M.H., Ramanathan, A., Gerszten, R.E., Wei, R., Fleming, M.D., Schreiber, S.L., and Cantley, L.C. (2008). The M2 splice isoform of pyruvate kinase is important for cancer metabolism and tumour growth. Nature *452*, 230–233.

Clower, C.V., Chatterjee, D., Wang, Z., Cantley, L.C., Vander Heiden, M.G., and Krainer, A.R. (2010). The alternative splicing repressors hnRNP A1/A2 and PTB influence pyruvate kinase isoform expression and cell metabolism. Proc. Natl. Acad. Sci. USA *107*, 1894–1899.

Dang, C.V., Le, A., and Gao, P. (2009). MYC-induced cancer cell energy metabolism and therapeutic opportunities. Clinical cancer research *15*, 6479–6483.

David, C.J., Chen, M., Assanah, M., Canoll, P., and Manley, J.L. (2010). HnRNP proteins controlled by c-Myc deregulate pyruvate kinase mRNA splicing in cancer. Nature *463*, 364–368.

Doi, D., Morizane, A., Kikuchi, T., Onoe, H., Hayashi, T., Kawasaki, T., Motono, M., Sasai, Y., Saiki, H., Gomi, M., et al. (2012). Prolonged maturation culture favors a reduction in the tumorigenicity and the dopaminergic function of human ESC-derived neural cells in a primate model of Parkinson's disease. Stem Cells *30*, 935–945.

Gao, P., Tchernyshyov, I., Chang, T.C., Lee, Y.S., Kita, K., Ochi, T., Zeller, K.I., De Marzo, A.M., Van Eyk, J.E., Mendell, J.T., and Dang, C.V. (2009). c-Myc suppression of miR-23a/b enhances mitochondrial glutaminase expression and glutamine metabolism. Nature *458*, 762–765.

Goldring, C.E., Duffy, P.A., Benvenisty, N., Andrews, P.W., Ben-David, U., Eakins, R., French, N., Hanley, N.A., Kelly, L., Kitteringham, N.R., et al. (2011). Assessing the safety of stem cell therapeutics. Cell Stem Cell *8*, 618–628.

Hanna, J., Wernig, M., Markoulaki, S., Sun, C.W., Meissner, A., Cassady, J.P., Beard, C., Brambrink, T., Wu, L.C., Townes, T.M., and Jaenisch, R. (2007). Treatment of sickle cell anemia mouse model with iPS cells generated from autologous skin. Science *318*, 1920–1923.

Hong, H., Takahashi, K., Ichisaka, T., Aoi, T., Kanagawa, O., Nakagawa, M., Okita, K., and Yamanaka, S. (2009). Suppression of induced pluripotent stem cell generation by the p53-p21 pathway. Nature *460*, 1132–1135.

Hussein, S.M., Batada, N.N., Vuoristo, S., Ching, R.W., Autio, R., Närvä, E., Ng, S., Sourour, M., Hämäläinen, R., Olsson, C., et al. (2011). Copy number variation and selection during reprogramming to pluripotency. Nature *471*, 58–62.

Jain, M., Arvanitis, C., Chu, K., Dewey, W., Leonhardt, E., Trinh, M., Sundberg, C.D., Bishop, J.M., and Felsher, D.W. (2002). Sustained loss of a neoplastic phenotype by brief inactivation of MYC. Science *297*, 102–104.

Kaji, K., Norrby, K., Paca, A., Mileikovsky, M., Mohseni, P., and Woltjen, K. (2009). Virus-free induction of pluripotency and subsequent excision of reprogramming factors. Nature *458*, 771–775.

Kriks, S., Shim, J.W., Piao, J., Ganat, Y.M., Wakeman, D.R., Xie, Z., Carrillo-Reid, L., Auyeung, G., Antonacci, C., Buch, A., et al. (2011). Dopamine neurons derived from human ES cells efficiently engraft in animal models of Parkinson's disease. Nature *480*, 547–551.

Lee, A.S., Tang, C., Rao, M.S., Weissman, I.L., and Wu, J.C. (2013). Tumorigenicity as a clinical hurdle for pluripotent stem cell therapies. Nat. Med. *19*, 998–1004.

Li, F., Wang, Y., Zeller, K.I., Potter, J.J., Wonsey, D.R., O'Donnell, K.A., Kim, J.W., Yustein, J.T., Lee, L.A., and Dang, C.V. (2005). Myc stimulates nuclearly encoded mitochondrial genes and mitochondrial biogenesis. Mol. Cell. Biol. *25*, 6225–6234.

Lin, C.H., Jackson, A.L., Guo, J., Linsley, P.S., and Eisenman, R.N. (2009). Myc-regulated microRNAs attenuate embryonic stem cell differentiation. EMBO J. *28*, 3157–3170.

Marión, R.M., Strati, K., Li, H., Murga, M., Blanco, R., Ortega, S., Fernandez-Capetillo, O., Serrano, M., and Blasco, M.A. (2009). A p53-mediated DNA

damage response limits reprogramming to ensure iPS cell genomic integrity. Nature *460*, 1149–1153.

Mayshar, Y., Ben-David, U., Lavon, N., Biancotti, J.-C., Yakir, B., Clark, A.T., Plath, K., Lowry, W.E., and Benvenisty, N. (2010). Identification and classification of chromosomal aberrations in human induced pluripotent stem cells. Cell Stem Cell *7*, 521–531.

Miura, K., Okada, Y., Aoi, T., Okada, A., Takahashi, K., Okita, K., Nakagawa, M., Koyanagi, M., Tanabe, K., Ohnuki, M., et al. (2009). Variation in the safety of induced pluripotent stem cell lines. Nat. Biotechnol. *27*, 743–745.

Nakagawa, M., Koyanagi, M., Tanabe, K., Takahashi, K., Ichisaka, T., Aoi, T., Okita, K., Mochiduki, Y., Takizawa, N., and Yamanaka, S. (2008). Generation of induced pluripotent stem cells without Myc from mouse and human fibroblasts. Nat. Biotechnol. *26*, 101–106.

Okita, K., Ichisaka, T., and Yamanaka, S. (2007). Generation of germline-competent induced pluripotent stem cells. Nature *448*, 313–317.

Osakada, F., Ikeda, H., Sasai, Y., and Takahashi, M. (2009). Stepwise differentiation of pluripotent stem cells into retinal cells. Nat. Protoc. *4*, 811–824.

Papapetrou, E.P., Lee, G., Malani, N., Setty, M., Riviere, I., Tirunagari, L.M., Kadota, K., Roth, S.L., Giardina, P., Viale, A., et al. (2011). Genomic safe harbors permit high β-globin transgene expression in thalassemia induced pluripotent stem cells. Nat. Biotechnol. *29*, 73–78.

Savino, M., Annibali, D., Carucci, N., Favuzzi, E., Cole, M.D., Evan, G.I., Soucek, L., and Nasi, S. (2011). The action mechanism of the Myc inhibitor termed Omomyc may give clues on how to target Myc for cancer therapy. PLoS ONE *6*, e22284.

Shim, H., Dolde, C., Lewis, B.C., Wu, C.S., Dang, G., Jungmann, R.A., Dalla-Favera, R., and Dang, C.V. (1997). c-Myc transactivation of LDH-A: implications for tumor metabolism and growth. Proc. Natl. Acad. Sci. USA *94*, 6658–6663.

Sodir, N.M., Swigart, L.B., Karnezis, A.N., Hanahan, D., Evan, G.I., and Soucek, L. (2011). Endogenous Myc maintains the tumor microenvironment. Genes Dev. *25*, 907–916.

Soucek, L., Helmer-Citterich, M., Sacco, A., Jucker, R., Cesareni, G., and Nasi, S. (1998). Design and properties of a Myc derivative that efficiently homodimerizes. Oncogene *17*, 2463–2472.

Soucek, L., Jucker, R., Panacchia, L., Ricordy, R., Tatò, F., and Nasi, S. (2002). Omomyc, a potential Myc dominant negative, enhances Myc-induced apoptosis. Cancer Res. *62*, 3507–3510.

Soucek, L., Whitfield, J., Martins, C.P., Finch, A.J., Murphy, D.J., Sodir, N.M., Karnezis, A.N., Swigart, L.B., Nasi, S., and Evan, G.I. (2008). Modelling Myc inhibition as a cancer therapy. Nature *455*, 679–683.

Stadtfeld, M., Apostolou, E., Akutsu, H., Fukuda, A., Follett, P., Natesan, S., Kono, T., Shioda, T., and Hochedlinger, K. (2010a). Aberrant silencing of imprinted genes on chromosome 12qF1 in mouse induced pluripotent stem cells. Nature *465*, 175–181.

Stadtfeld, M., Maherali, N., Borkent, M., and Hochedlinger, K. (2010b). A reprogrammable mouse strain from gene-targeted embryonic stem cells. Nat. Methods *7*, 53–55.

Takahashi, K., and Yamanaka, S. (2006). Induction of pluripotent stem cells from mouse embryonic and adult fibroblast cultures by defined factors. Cell *126*, 663–676.

Takebe, T., Sekine, K., Enomura, M., Koike, H., Kimura, M., Ogaeri, T., Zhang, R.R., Ueno, Y., Zheng, Y.W., Koike, N., et al. (2013). Vascularized and functional human liver from an iPSC-derived organ bud transplant. Nature *499*, 481–484.

Tan, H.L., Fong, W.J., Lee, E.H., Yap, M., and Choo, A. (2009). mAb 84, a cytotoxic antibody that kills undifferentiated human embryonic stem cells via oncosis. Stem Cells *27*, 1792–1801.

Vander Heiden, M.G., Cantley, L.C., and Thompson, C.B. (2009). Understanding the Warburg effect: the metabolic requirements of cell proliferation. Science *324*, 1029–1033.

Varlakhanova, N., Cotterman, R., Bradnam, K., Korf, I., and Knoepfler, P.S. (2011). Myc and Miz-1 have coordinate genomic functions including targeting Hox genes in human embryonic stem cells. Epigenetics & chromatin *4*, 20.

von Eyss, B., and Eilers, M. (2011). Addicted to Myc—but why? Genes Dev. *25*, 895–897.

Weinstein, I.B. (2002). Cancer. Addiction to oncogenes—the Achilles heal of cancer. Science *297*, 63–64.

Werbowetski-Ogilvie, T.E., Bossé, M., Stewart, M., Schnerch, A., Ramos-Mejia, V., Rouleau, A., Wynder, T., Smith, M.J., Dingwall, S., Carter, T., et al. (2009). Characterization of human embryonic stem cells with features of neoplastic progression. Nat. Biotechnol. *27*, 91–97.

Wernig, M., Meissner, A., Cassady, J.P., and Jaenisch, R. (2008). c-Myc is dispensable for direct reprogramming of mouse fibroblasts. Cell Stem Cell *2*, 10–12.

Wu, C.H., van Riggelen, J., Yetil, A., Fan, A.C., Bachireddy, P., and Felsher, D.W. (2007). Cellular senescence is an important mechanism of tumor regression upon c-Myc inactivation. Proc. Natl. Acad. Sci. USA *104*, 13028–13033.

Yang, W., Xia, Y., Hawke, D., Li, X., Liang, J., Xing, D., Aldape, K., Hunter, T., Alfred Yung, W.K., and Lu, Z. (2012). PKM2 phosphorylates histone H3 and promotes gene transcription and tumorigenesis. Cell *150*, 685–696.

Zhang, J., Khvorostov, I., Hong, J.S., Oktay, Y., Vergnes, L., Nuebel, E., Wahjudi, P.N., Setoguchi, K., Wang, G., Do, A., et al. (2011). UCP2 regulates energy metabolism and differentiation potential of human pluripotent stem cells. EMBO J. *30*, 4860–4873.

Zhang, J., Nuebel, E., Daley, G.Q., Koehler, C.M., and Teitell, M.A. (2012). Metabolic regulation in pluripotent stem cells during reprogramming and self-renewal. Cell Stem Cell *11*, 589–595.